Asymptotics of diffraction corrections in radiometry

Eric Shirley
Remote Sensing Group
Sensor Science Division, NIST

Presentation Outline:

- Background
- 3-element systems (1 aperture)
- Solar radiometry example
- Multistage systems
- Recent innovations
- Summary

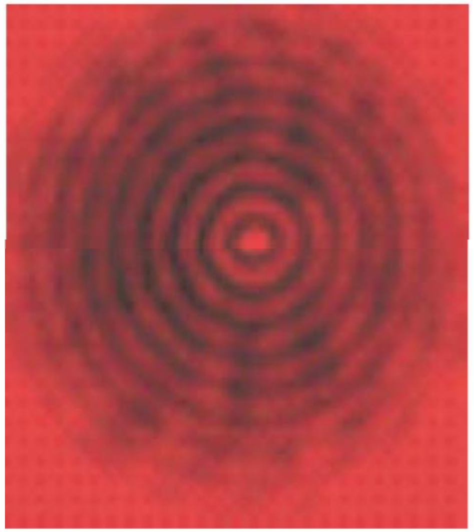

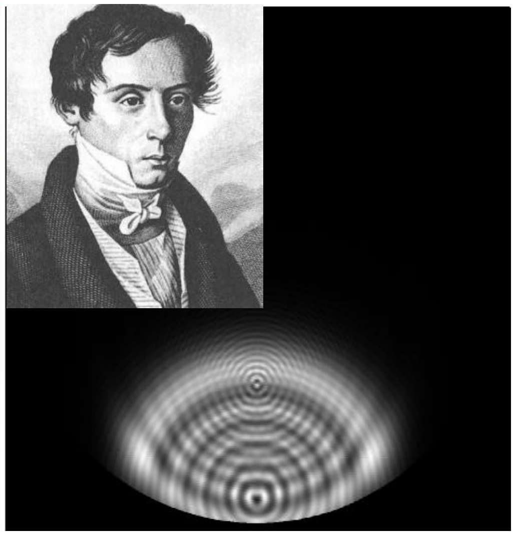

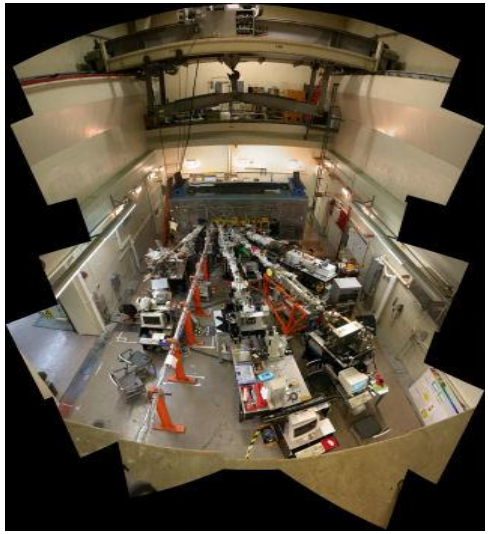

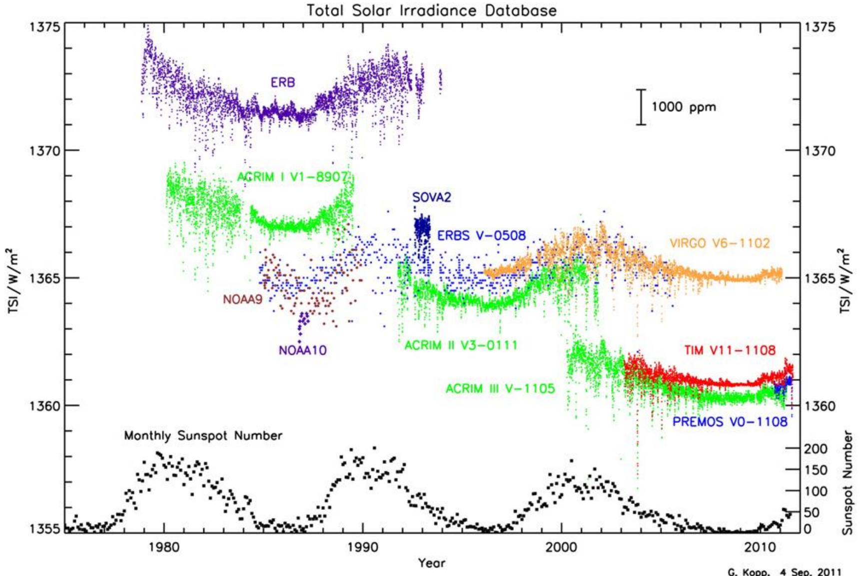

Some prior work diffraction effects in radiometry:

Theory:

Rayleigh (*Phil. Mag.* **11**, 214, 1881): Rayleigh formula $1 - J_0^2(v) - J_1^2(v)$

E. Lommel (*Abh. Bayer. Akad.* **15**, 233, 1885): Fresnel diffraction, unfocussed

E. Wolf (Proc. Roy. Soc. A **204**, 533, 1951)

J. Focke (*Optica* Acta **3**, 161, 1956)

Radiometry (mostly at NMIs):

C.L. Sanders and O.C. Jones (*J. Opt. Soc. Am.* **52**, 731, 1962)

N. Ooba (*J. Opt. Soc. Am.* **54**, 357, 1964)

W.R. Blevin (*Metrologia* **6**, 39, 1970): effective-wavelength approximation

W.H. Steel, M. De, and J.A. Bell (*J. Opt. Soc. Am.* **62**, 1099, 1972): extended source

L.P. Boivin (*Appl. Opt.* **14**, 197; **14**, 2002; **15**, 1204, **16**, 377, 1972-1977): general

Physical optics: key approximations

- Scalar-wave approximation
- Kirchhoff diffraction theory, cont'd.
- Fresnel-paraxial (Gaussian optics) approx.

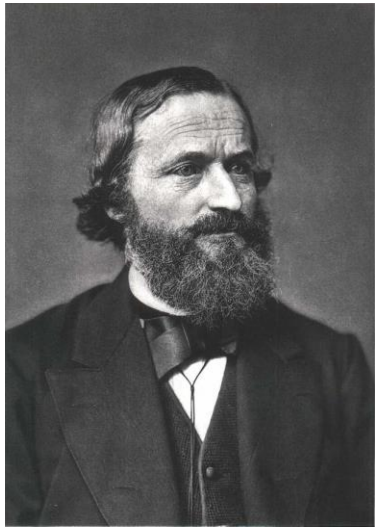

Gustav Kirchhoff

Consider this optical system:

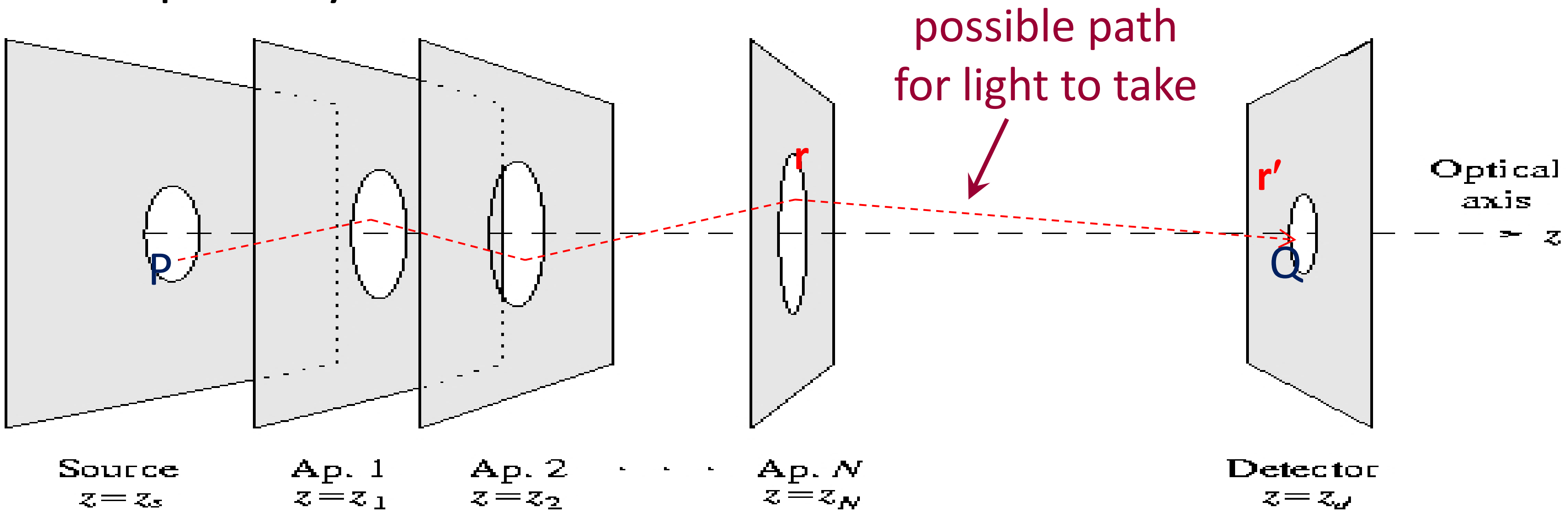

Repeated application of approximations gives

$$u(\mathbf{Q}) = \frac{1}{(i\lambda)^N} \int_{A_1} dx_1\, dy_1 \ldots \int_{A_N} dx_N\, dy_N\; G(\mathbf{P},\mathbf{x}_1)\cdots G(\mathbf{x}_N,\mathbf{Q}) \cdot \exp[i\textstyle\sum_k \delta l_k(\mathbf{x}_k)]$$

Allows for focusing effects

Identification of 3-element subsystems:

SAD subsystems:

SAD:
source-aperture-detector

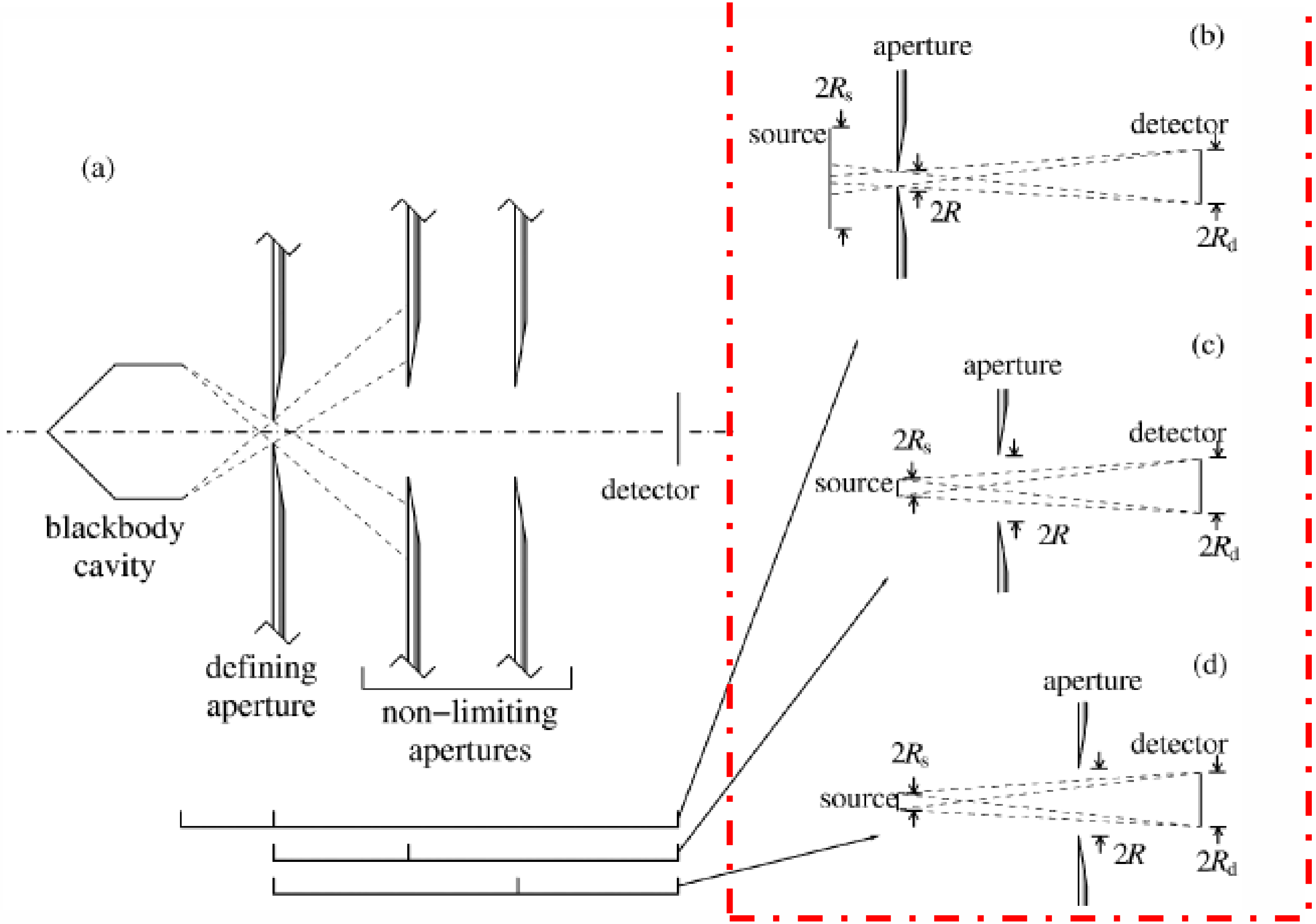

FIG. 9.7. Optical setup conceptually treated as three SAD setups for purposes of diffraction effects.

Diffraction Effect in SAD systems (point source)

$$L = \frac{\text{flux on detector}}{\text{flux on aperture}}$$

v, u, w (& A): depend on geometry, focusing power (& temperature)

Limiting geometries

$$w^2 = \begin{array}{l}\text{geometrically}\\ \text{illuminated}\\ \text{fraction of}\\ \text{detector area}\end{array}$$

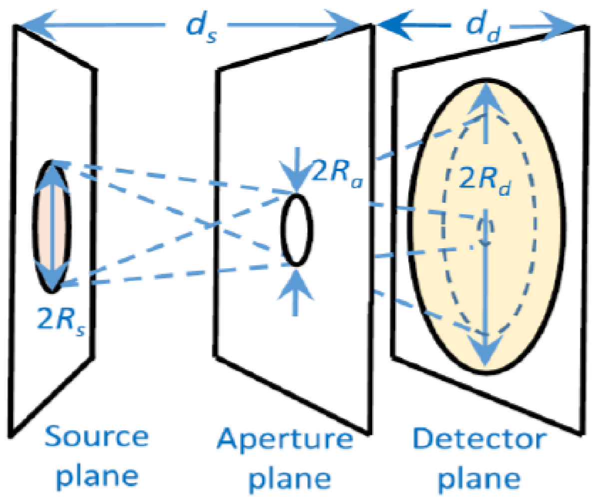

Spectral case:

$$L = 1 - L_B(v, w)$$

Thermal case:

$$L = 1 - \frac{A^4}{6\zeta(4)} F_B(A, w)$$

Non-limiting geometries

$$w^2 = \begin{array}{l}\text{geometrical}\\ \text{value of } L\end{array}$$

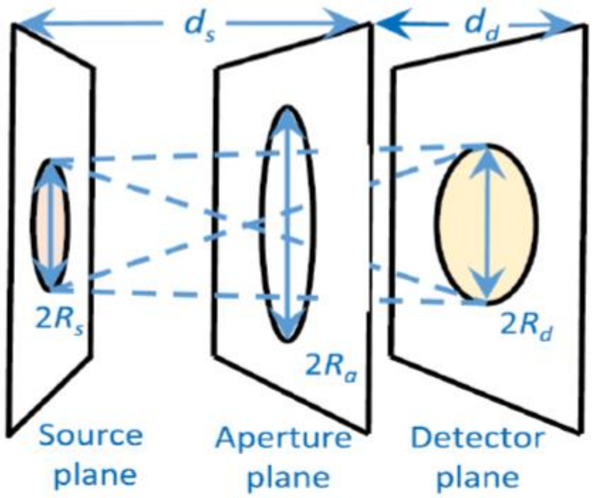

Spectral case:

$$\frac{L}{w^2} = 1 + L_B(v, w) - \frac{1}{w^2} L_X(v, w)$$

Thermal case:

$$\frac{L}{w^2} = 1 + \frac{A^4}{6\zeta(4)} \left[F_B(A, w) - \frac{1}{w^2} F_X(A, w) \right]$$

- Integral representation of $L_B(v,w)$, $L_X(v,w)$, $F_B(A,w)$ and $F_X(A,w)$
  - **asymptotic expansions** (large v, small A)
  - **exact evaluation by appropriate quadrature** (large v, small A)
  - generalizable to **extended sources**…
- Sample asymptotic results for a point source:

$$L_B(v,w) \sim \frac{1}{\pi}\left[\frac{2}{v(1-w^2)} - \frac{\cos(2v)}{v^2(1-w^2)} + \frac{1-20w^2-90w^4-20w^6+w^8}{4v^3(1-w^2)^5} - \frac{(1-18w^2+w^4)\sin(2v)}{4v^3(1-w^2)^5} + \ldots\right]$$

$$F_B(A,w) \sim \frac{4\zeta(3)}{\pi(1-w^2)}A^{-3} - \left(\frac{1-20w^2-90w^4-20w^6+w^8}{4\pi(1-w^2)^5}\right)\left(A^{-1}\log_e A - \frac{2\gamma+6\log_e 2+11/3}{2}A^{-1}\right) + \left[-\frac{5w^8-112w^6-586w^4-112w^2+5}{6\pi(1-w^2)^5} + \frac{32w^3(1+w^2)}{\pi(1-w^2)^5}\log_e\left(\frac{1+w}{1-w}\right)\right]A^{-1} + \ldots$$

- Palindromic polynomials at **all orders**, as well as in $L_X(v,w)$ and $F_X(A,w)$.
- In particular, consider small-λ form for spectral power:

Limiting case:

$$\frac{\Phi_\lambda(\lambda)}{\Phi_\lambda^0(\lambda)} \approx 1 - \lambda a_0'(\lambda) - \lambda^{7/2}\{a_B'(\lambda) + [a_B'(\lambda)]^*\}$$

Non-limiting case:

$$\frac{\Phi_\lambda(\lambda)}{\Phi_\lambda^0(\lambda)} \approx 1 + \lambda a_0(\lambda) + \lambda^{7/2}\{a_B(\lambda) + [a_B(\lambda)]^*\} + \lambda^3\{a_X(\lambda) + [a_X(\lambda)]^*\}$$

All a-functions involve trivial phase factors and smooth functions of λ, facilitating interpolation over wavelengths where integral representations are more practical than exact numerical evaluation!

Extended sources:

Generalizations of all previous results are also in hand.

General formula—

$$\Phi = C\int_{-1}^{+1} dx\, \frac{\{(1-x^2)[(2+\sigma x)^2-\sigma^2]\}^{1/2}}{1+\sigma x}\int_0^{\infty} d\lambda\, L(u,v)L_\lambda(\lambda)$$

$$C = 4\pi^3 R_a^4 R_s^2 R_d^2 / (d_s^2 d_d^2 \alpha_0^2)^2 \quad \text{(depends on geometry)}$$

W.H. Steel *et al.*, *J. Opt. Soc. Am.* **62**, 1099 (1972)
L.P. Boivin, *Appl. Opt.* **15**, 1204 (1976)
E.L. Shirley, *Appl. Opt.* **37**, 6581 (1998), *JOSA A* **21**, 1895 (2004);
JOSA A **33**, 1509 (2016)

P. Edwards and M. McCall,
Appl. Opt. ***42***, 5024 (2003)—treats more geometries

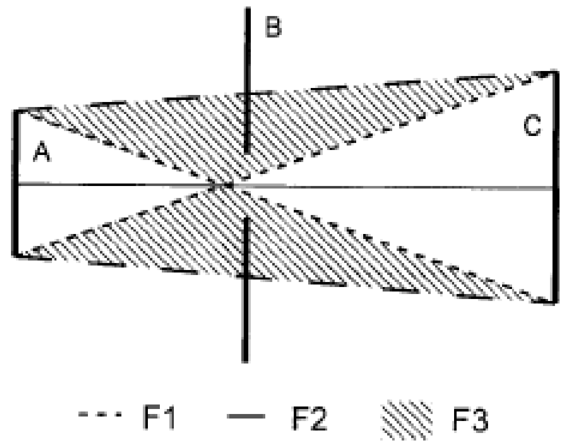

Principle of measuring total solar irradiance:

(1.) Have an aperture of known area

(2.) Measure *total* power passing through that aperture

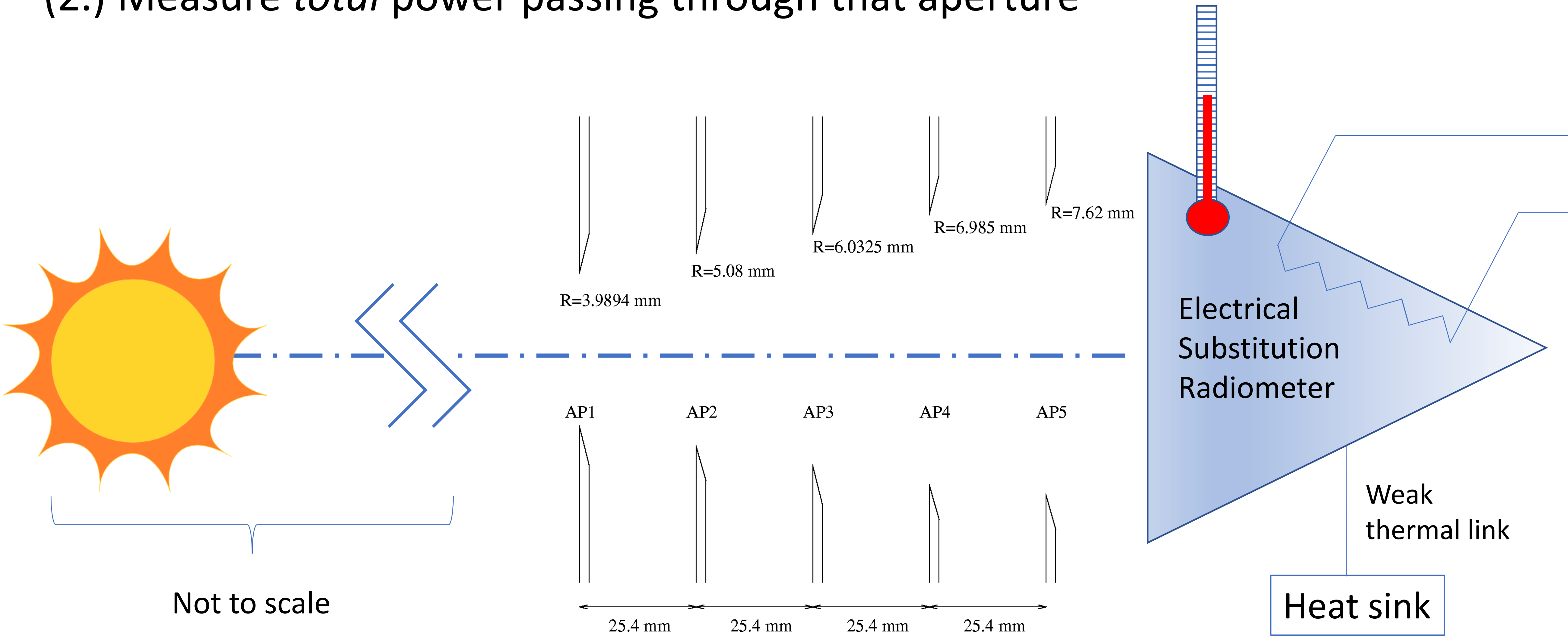

Sources of Differences in On-Orbital Total Solar Irradiance Measurements and Description of a Proposed Laboratory Intercomparison

Volume 113 | Number 4 | July-August 2008

J. J. Butler

National Aeronautics and Space Administration,
Goddard Space Flight Center,
Greenbelt, MD

B. C. Johnson, J. P. Rice, and E. L. Shirley

National Institute of Standards and Technology,
Gaithersburg, MD 20899-0000

and

R. A. Barnes

SAIC,

There is a 5 W/m^2 (about 0.35 %) difference between current on-orbit Total Solar Irradiance (TSI) measurements. On 18-20 July 2005, a workshop was held at the National Institute of Standards and Technology (NIST) in Gaithersburg, Maryland that focused on understanding possible reasons for this difference, through an examination of the instrument designs, calibration approaches, and appropriate measurement equations. The instruments studied in that workshop included the Active Cavity Radiometer Irradiance Monitor III (ACRIM III) on the Active Cavity Radiometer Irradiance Monitor SATellite (ACRIMSAT), the Total Irradiance Monitor (TIM) on the Solar Radiation and Climate Experiment (SORCE), the Variability of solar IRradiance and Gravity Oscillations (VIRGO) on the Solar and Heliospheric Observatory (SOHO), and the Earth

a session on laboratory-based comparisons and the application of new laboratory comparison techniques. The workshop has led to investigations of the effects of diffraction and of aperture area measurements on the differences between instruments. In addition, a laboratory-based instrument comparison is proposed that uses optical power measurements (with lasers that underfill the apertures of the TSI instruments), irradiance measurements (with lasers that overfill the apertures of the TSI instrument), and a cryogenic electrical substitution radiometer as a standard for comparing the instruments. A summary of the workshop and an overview of the proposed research efforts are presented here.

Key words: absolute radiometric calibration; diffraction calculations; total solar

Sources of Differences in On-Orbital Total Solar Irradiance Measurements and Description of a Proposed

Volume 113

J. J. Butler

National Aero
Administratio
Goddard Spac
Greenbelt, MD

B. C. Johnson
E. L. Shirley

National Instit
and Technolog
Gaithersburg,

and

R. A. Barnes

SAIC,
Beltsville, MD

Radiation and Climate Experiment (SORCE), the Variability of solar IRradiance and Gravity Oscillations (VIRGO) on the Solar and Heliospheric Observatory (SOHO), and the Earth Radiation Budget Experiment (ERBE) on

are presented here.

Key words: absolute radiometric calibration; diffraction calculations; total solar irradiance (TSI); TSI uncertainty; TSI

IOP PUBLISHING METROLOGIA

Metrologia **49** (2012) S29–S33 doi:10.1088/0026-1394/49/2/S29

Total solar irradiance data record accuracy and consistency improvements

Greg Kopp[1], André Fehlmann[2], Wolfgang Finsterle[2], David Harber[1], Karl Heuerman[1] and Richard Willson[3]

[1] Laboratory for Atmospheric and Space Physics, University of Colorado, Boulder, CO 80303, USA
[2] Physikalisch-Meteorologisches Observatorium Davos/World Radiation Center, Davos, Switzerland
[3] ACRIM, 12 Bahama Bend, Coronado, CA 92118, USA

IOP Publishing — Metrologia

Metrologia **49** (2012) S29–S33 — doi:10.1088/0026-1394/49/2/S29

Total solar irradiance data record ac

Greg

Karl

[1] Labora

[2] Physik

[3] ACRI

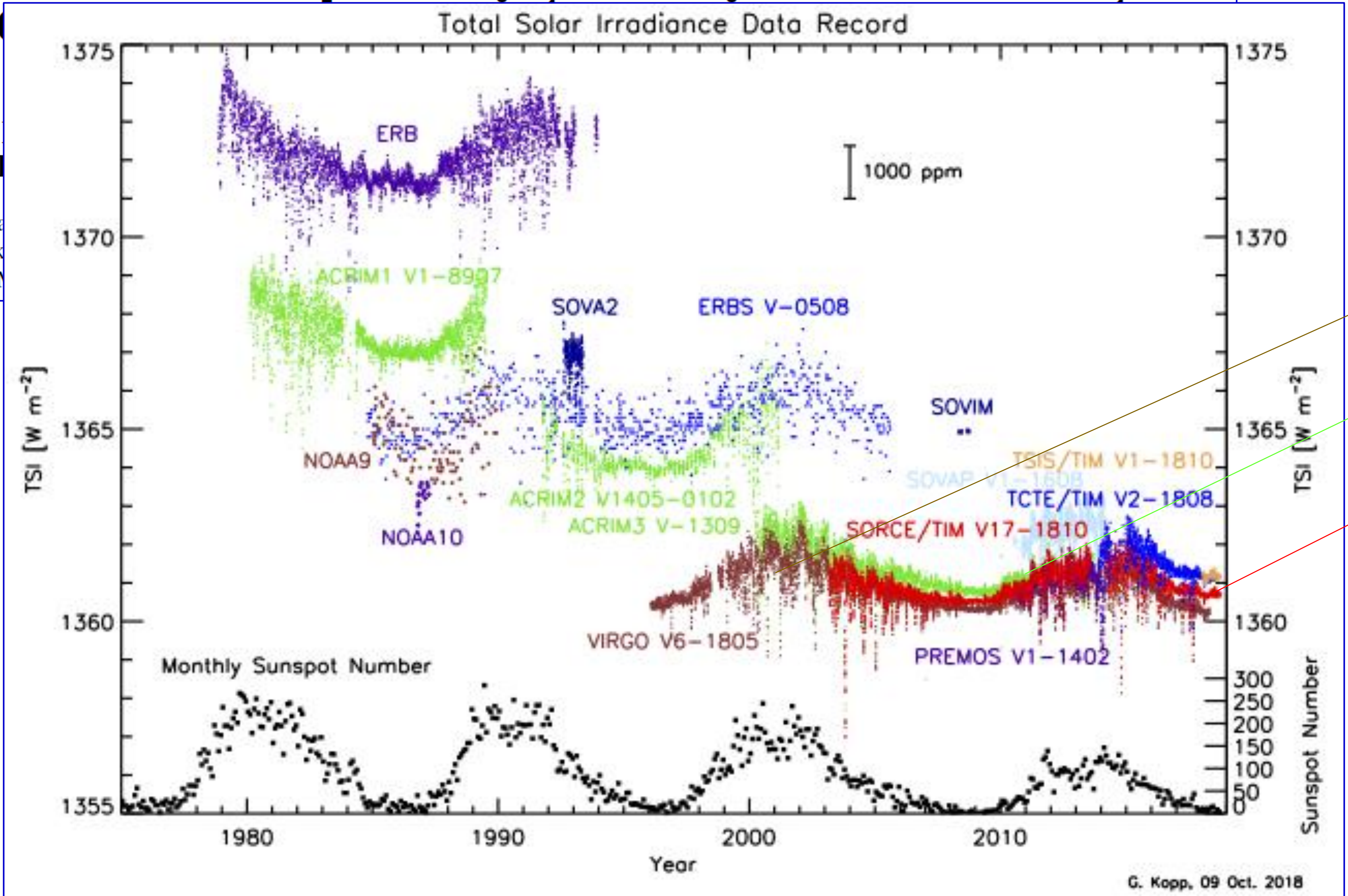

Corrected for
0.12% diffraction gain

Corrected for
0.16% diffraction gain

Corrected for
0.04% diffraction loss

0.02% decadal variation in TSI relevant to understanding climate change!

LASP SORCE/TIM instrument

Application of algorithmic speedups to calculation of diffraction-corrected throughput of a multi-stage solar radiometer:

BEFORE FFT TRICK (also, using 10.0 GB memory):

```
   0.902000000000000E-03  0.762000000000048E+01  0.317948922457192E-02    cap
47570.374u 12.473s 1:44:52.68 756.1%  0+0k 0+50624io 0pf+0w
```

AFTER FFT TRICK* (also, using 1.3 GB memory):

```
   0.902000000000000E-03  0.762000000000048E+01  0.317948922456555E-02    cap
678.938u 1.529s 11:20.24 100.0%  0+0k 0+13744io 0pf+0w
```

* J.S. Rubin, *et al.*, *Appl. Opt.* **57**, 788 (2018)

Beyond the SAD paradigm:

- Multistage optics trains
- Vignetting effects

One-edge effects:

→ corrections proportional to λ or $1/T$.

Two-edge effects (most important for source-pinhole-baffle-detector cases):

→ corrections proportional to λ^2 or $1/T^2$.

Example: blackbody calibration in NIST's Low-background infrared facility:

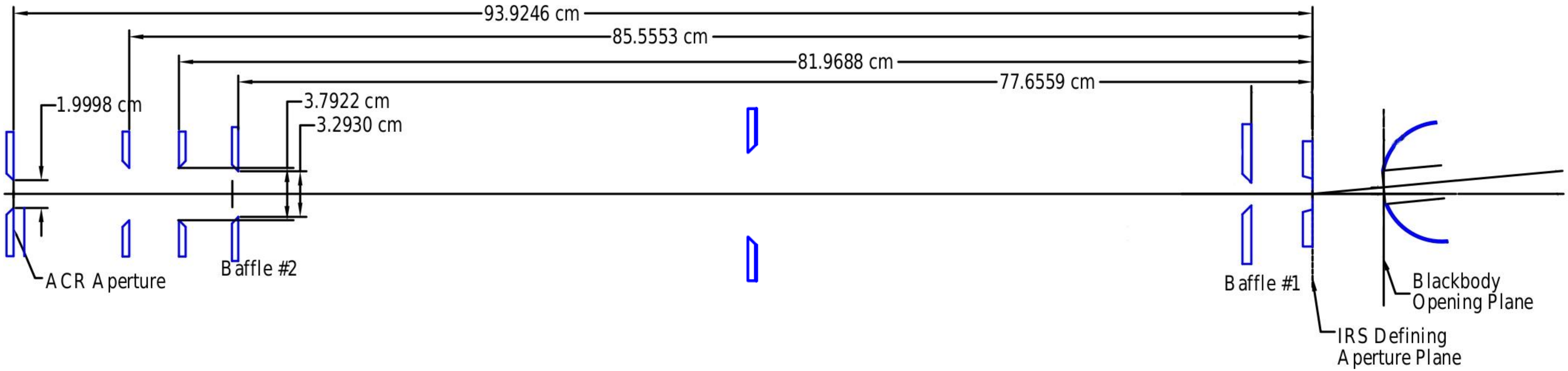

Some 3-element subsystems can be treated for total or spectral power diffraction effects efficiently. We are moving to treating other effects more **automatically.**

Light that is diffracted twice…

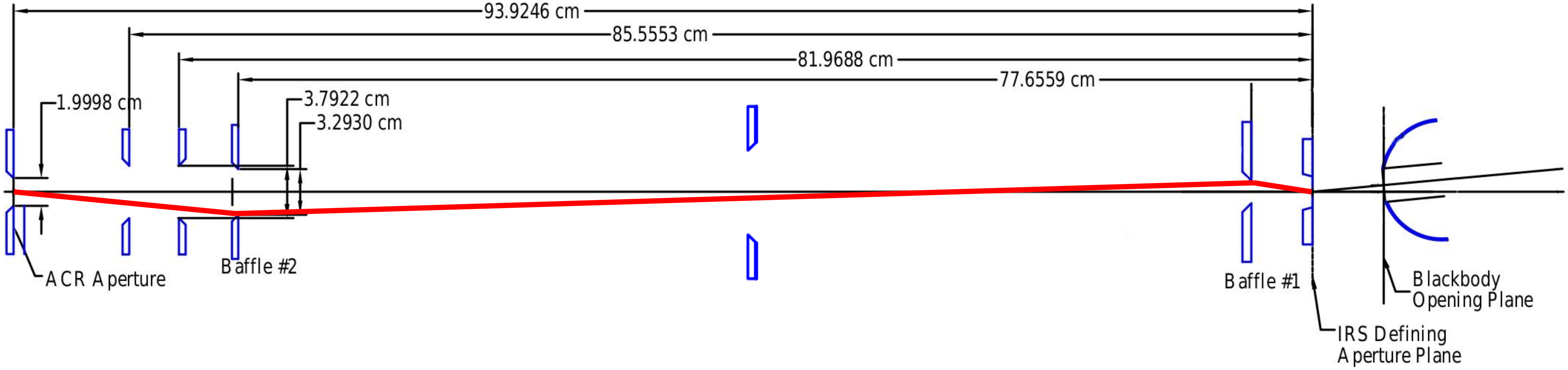

Light that is diffracted twice…2nd bounce might be on an aperture normally not illuminated

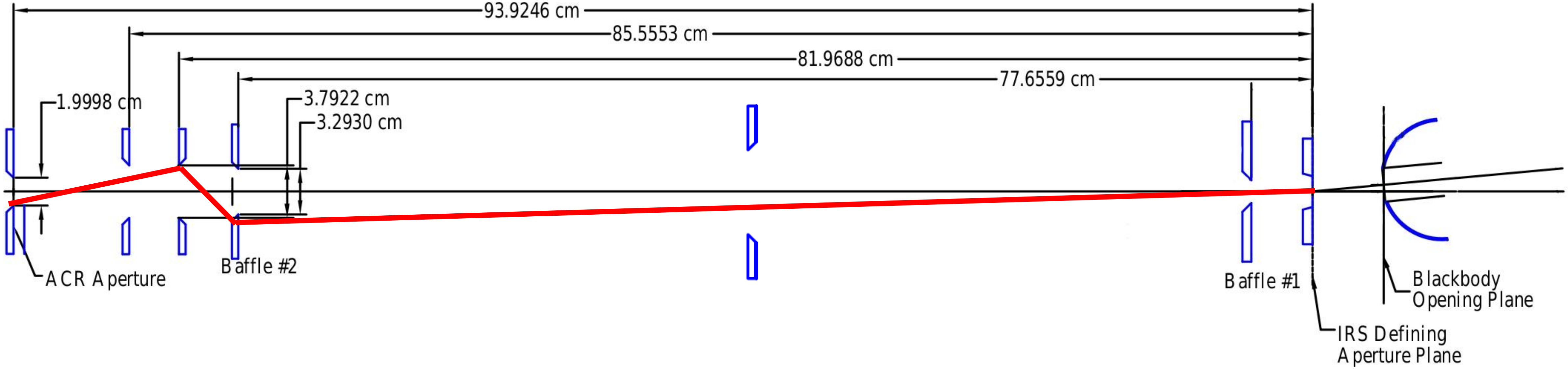

Light that should be diffracted 1x might be reduced by diffraction at BB pinhole aperture

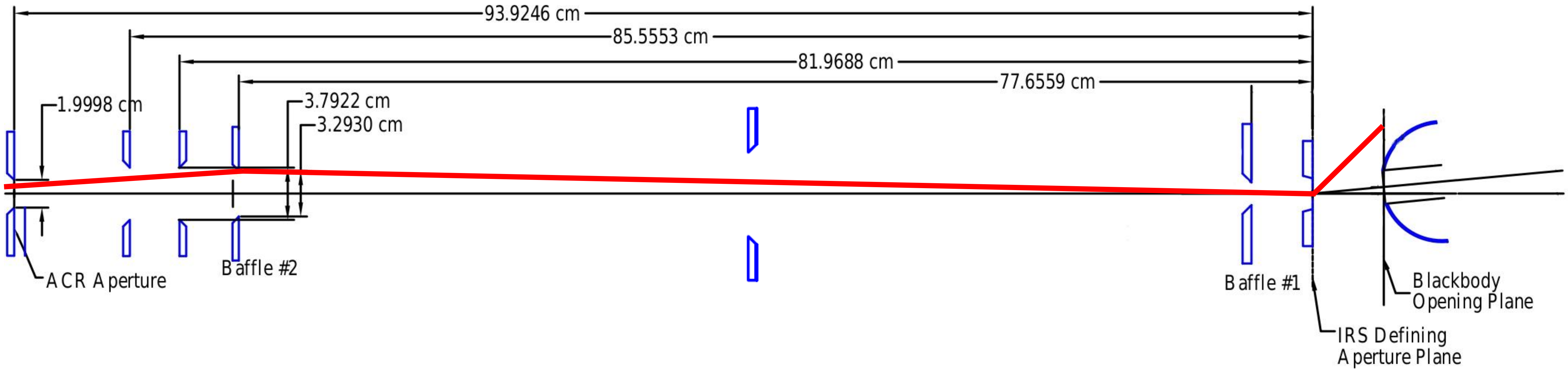

A baffle nominally not illuminated might diffract light after the pinhole diffracts it on the baffle edge…

In another context, having a blackbody recessed from the S of a SAD combination can also have a secondary effect

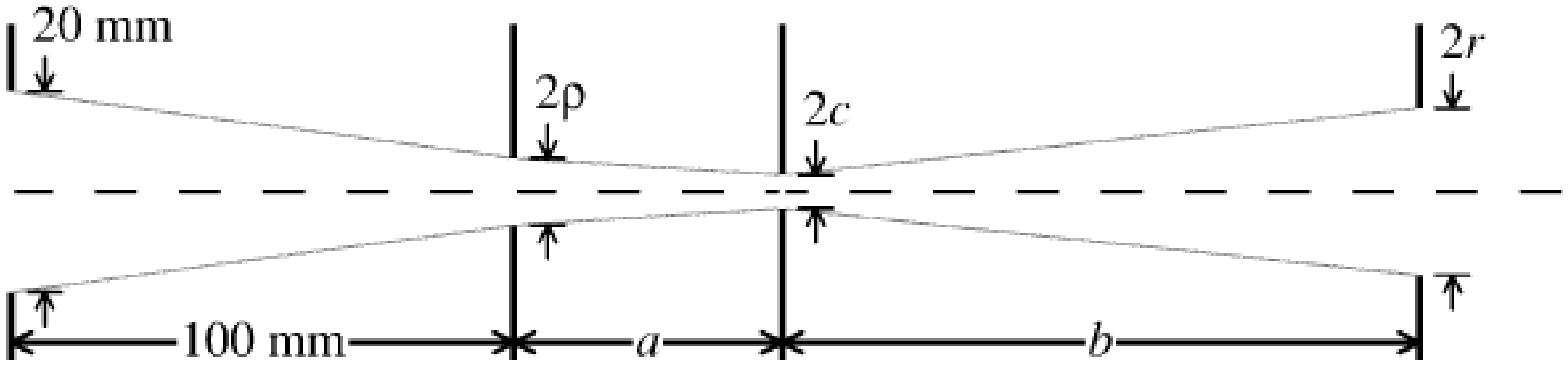

Treatment of a multi-stage system, in practice:

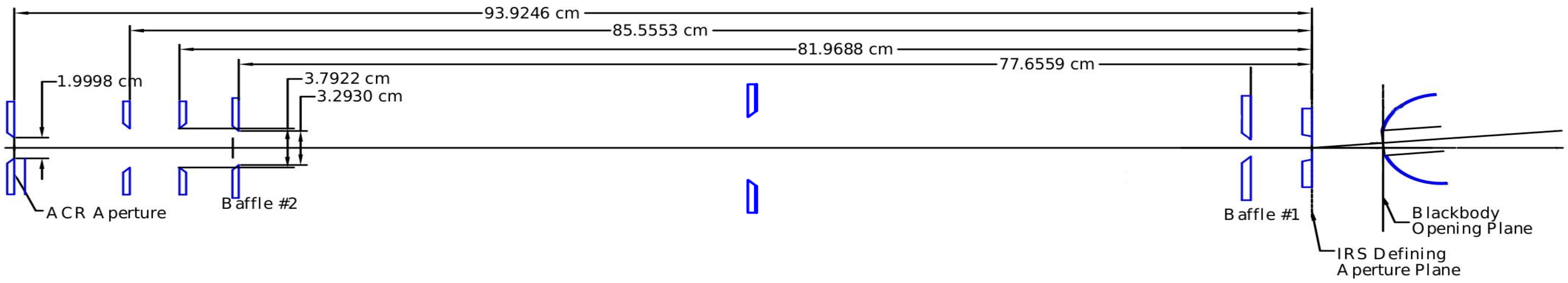

At small wavelength, one can show*

$$\frac{\Phi_\lambda(\lambda)}{\Phi_{0,\lambda}(\lambda)} = 1 + a_1\lambda + a_2\lambda^2 + R_\lambda(\lambda)$$

(a_1,a_2)=analytic

$$R_\lambda(\lambda) = \begin{cases} \text{neglected for } \lambda < \lambda_m \\ \text{computed for } \lambda \geq \lambda_m \end{cases}$$

At high temperature, one can show*

$$\frac{\Phi}{\Phi_0} = 1 + \frac{b_1}{T} + \frac{b_2}{T^2} + R_T(T)$$

(b_1,b_2)=analytic

$$R_T(T) \sim \frac{b_3}{T^3} \text{ at large } T \text{ (usually)}$$

*Based on an extended boundary-diffraction-wave formulation; E. L. Shirley, J. Mod. Opt. 54, 515 (2007)

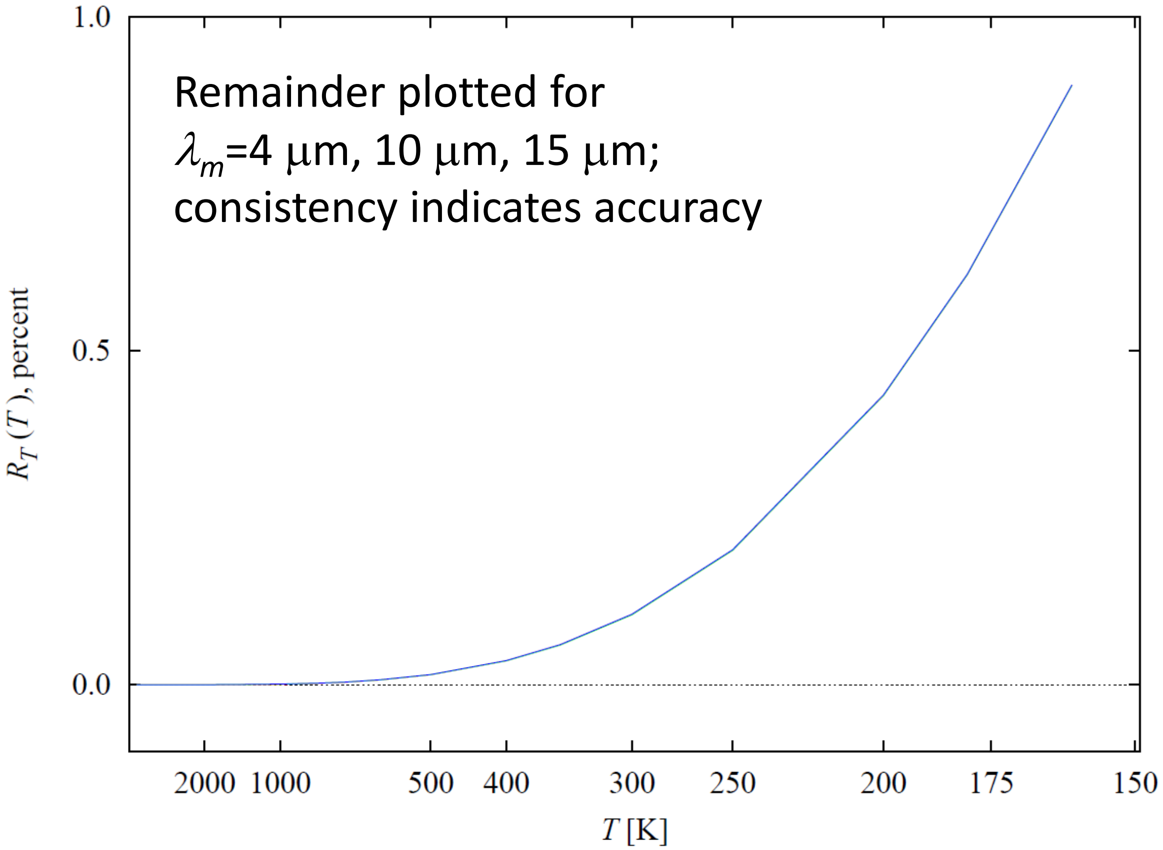

Comparison of measured and calculated diffraction effects:

L.P. Boivin, (*Appl. Opt.* **17**, 3323, 1978)

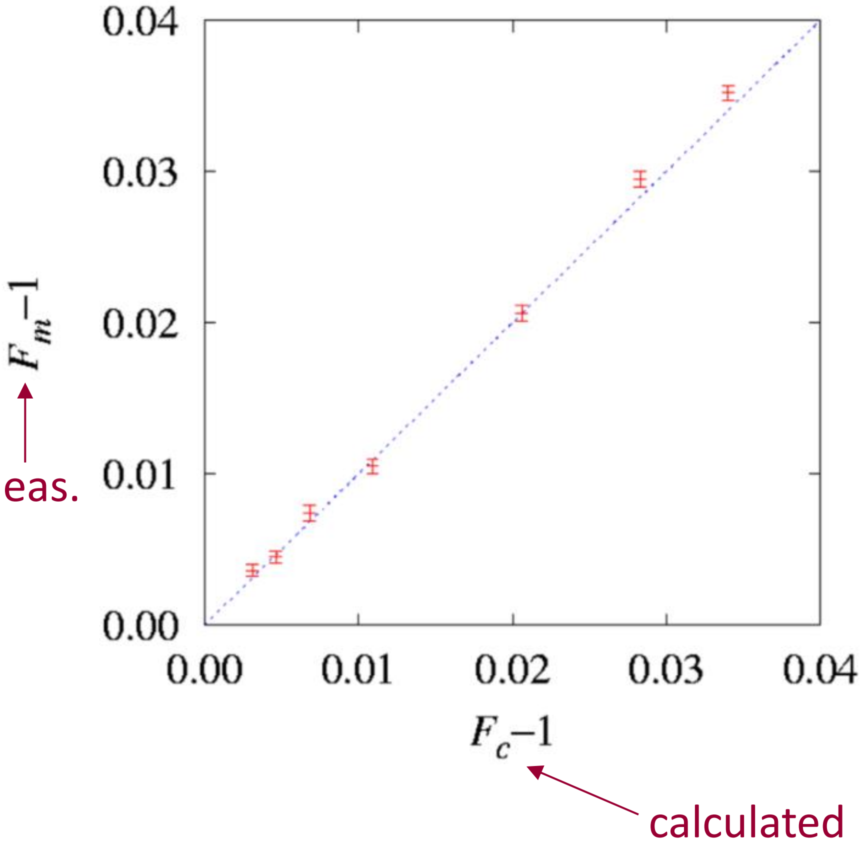

Statistical analysis suggests ~2 % systematic error in calculated diffraction corrections.

Effect of toothing of aperture:

- reduction in diffraction effect because of phase cancellations in $u_{BDW}(\mathbf{r}_d)$.

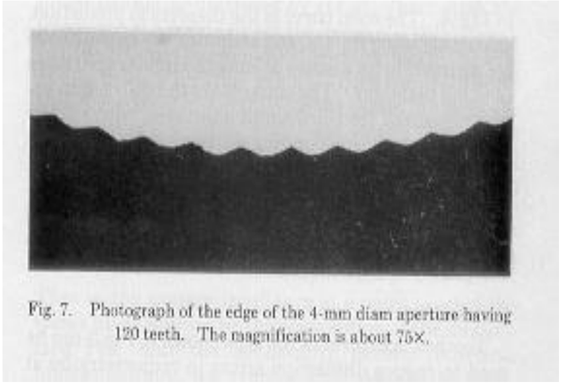

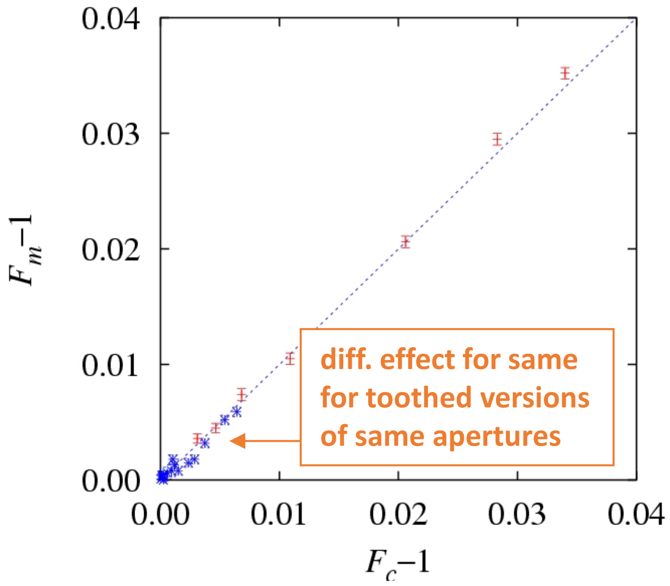

Summary of results:

- Diffraction affects radiometry
- Largely understood
- Much work has been done
- We have programs that are efficient and pull out asymptotic trends, easing or obviating calculations
- Codes are ever more efficient, and are available